

If the geometry is tetrahedral, among 3d orbitals of the highest energy, the  $3d_{xz}$  orbital can form  $\pi$ -bonding with the  $\pi$ -system of SQ (Figure 5 (right)). Since all 3d orbitals are doubly occupied, while  $MO_{ue}$  is singly occupied, there are two electrons on the bonding orbital and one in the antibonding orbital, if a covalent bond is formed. Consequently, the net electronic charge changes in the direction opposite to that of the spin density: the transfer of  $3d_{xz}$  electron pair from the metal ion into SQ is accompanied by the transfer of an unpaired electron from SQ to the metal ion. In particular, if a substituent enlarges the electron affinity of SQ, then its negative charge density increases and its spin density decreases, while the variation of these densities takes place in the opposite direction on the metal ion and neutral ligands. Con-

cerning the spin distribution on the SQ skeleton, the spin density is large on those atoms where the charge density is enhanced owing to the  $3d_{xz}$  electron pair transport. The larger spin transfer in the complexes  $[Cu(SQ)L_2]$  than in the complexes  $[Cu(SQ)L]$  can also be explained in our model: the energy of the  $3d_{xz}$  orbital is much larger in the tetrahedral ligand field than in the trigonal field, which makes the separation of  $3d_{xz}$  and  $MO_{ue}$  orbitals smaller and the respective  $\pi$ -bond stronger, and consequently, more charge is transported to SQ and more spin density to the metal ion and neutral ligands.

Registry No. 1, 65123-87-7; 2, 109959-92-4; 3, 109959-93-5; 4, 109959-94-6; 5, 109959-95-7; 6, 109959-96-8; 7, 109959-97-9.

Contribution from the Department of Chemistry and Ipatieff Catalytic Laboratory, Northwestern University, Evanston, Illinois 60201

## Synthesis of Lithium Dialuminate by Salt Imbibition

K. R. Poeppelmeier\* and S.-J. Hwu

Received December 30, 1986

The synthesis of lithium dialuminate  $LiAl_2(OH)_7 \cdot 2H_2O$  by reaction at room temperature of solid lithium hydroxide, polycrystalline aluminum trihydroxide (bayerite), and water vapor is described. The aluminate prepared by this method has been characterized by chemical analysis, thermogravimetric analysis, infrared spectroscopy, and X-ray powder diffraction and appears to be identical with that prepared by precipitation from supersaturated aluminate solutions or by reaction of lithium salts with freshly precipitated aluminum hydroxide in aqueous solution. All current evidence suggests that the structure of lithium dialuminate is like that of hydrotalcite,  $[Mg_6Al_2(OH)_{16}]^{2+}CO_3^{2-} \cdot 4H_2O$ , with neutral dioctahedral sheets of bayerite converted to positively charged trioctahedral layers by incorporation of lithium ion. Hydroxide ion and two water molecules reside between the layers and presumably approximate a plane of oxygen atoms stabilized by hydrogen bonding, as evidenced by a 2.81 (1) Å increase in the bayerite lattice perpendicular to the dioctahedral layer. A more descriptive chemical formula for lithium dialuminate would be  $[LiAl_2(OH)_6]^+OH^- \cdot 2H_2O$ . The imbibition of other lithium salts ( $LiX$ ;  $X = Cl^-, Br^-, I^-, NO_3^-$ ) was also studied. Thermal decomposition results in compounds, related to the transitional aluminas, with high specific surface area and porosity.

### Introduction

Hydrated lithium dialuminate,  $LiAl_2(OH)_7 \cdot 2H_2O$ , precipitates<sup>1</sup> from a solution prepared by dissolving aluminum metal in hot lithium hydroxide and was originally formulated to be an "acid" aluminate  $LiH(AlO_2)_2 \cdot 5H_2O$ . Subsequent investigators used conductometric measurements to study the soluble species  $Al(OH)_4^-$  and  $Al_2(OH)_7^-$  and suggested<sup>2</sup> that the formula should reflect two molecules of water loosely bound as waters of crystallization, with the remaining water bound directly to the aluminum cations. Later it was shown<sup>3</sup> that pH and lithium ion concentration could be varied over a considerable range without an effect on the composition of the insoluble compound. Recently<sup>4</sup> it has been shown that the dialuminate compound  $LiAl_2(OH)_7 \cdot 2H_2O$  is not the only compound that can be isolated from aqueous solution. The reaction of hydrated lithium dialuminate at 90 °C with a concentrated sodium hydroxide solution is reported to result in crystalline lithium monoaluminate with the approximate chemical composition  $Li_2O \cdot Al_2O_3 \cdot nH_2O$  with  $n \sim 0.5$ .

Of considerable technological importance are factors that determine the nature of the particular aluminum hydroxide phase to precipitate from solution such as the type and amount of alkali-metal ion present, temperature, and pH. Bayerite and pseudoboehmite are precipitated in the presence of  $Na^+$ ,  $K^+$ , and  $Cs^+$  ions. In the presence of  $Li^+$  ions<sup>5,6</sup> pseudoboehmite does not readily form, and a selective and accelerated precipitation of bayerite is observed at low  $Li^+$  ion concentrations, whereas at low

supersaturation and high  $Li^+$  concentrations bayerite formation is preceded by  $LiAl_2(OH)_7 \cdot 2H_2O$  precipitation.

Powder X-ray diffraction patterns have been reported for both the mono- and dialuminates.<sup>4,7</sup> Recently a structural model that does not require all the hydroxide ions to be bound to the aluminum cations has been proposed<sup>8</sup> for the hydrated lithium dialuminate. In a study of the hydrolysis of  $Al^{3+}$  in carbonate salt solutions the compound  $[LiAl_2(OH)_6]_2^+CO_3^{2-} \cdot nH_2O$  was isolated. On the basis of electron diffraction, X-ray powder diffraction, and infrared studies, it was suggested that these dialuminates are derivatives of  $Al(OH)_3$  where aluminum cations occupy two-thirds of the octahedral sites between sheets of close-packed hydroxide ions and lithium cations fill the remaining octahedral sites (one-third). That is, the compound  $LiAl_2(OH)_7 \cdot 2H_2O$  is a layered double hydroxide. The more descriptive formula  $[LiAl_2(OH)_6]^+OH^- \cdot 2H_2O$  emphasizes the fact that the one additional hydroxide ion is an interlayer anion. Ideally, two molecules of water also occupy the interlayer region in this compound.

Because the structure of these hydrotalcite-like compounds are conceptually derived from that of crystalline  $Al(OH)_3$  (e.g., bayerite), we considered the direct reaction of  $LiOH \cdot H_2O(s)$  with  $Al(OH)_3(s)$ . Reactions of alumina gels (gibbsite, bayerite, or norstandite) with lithium salts in aqueous media have been reported.<sup>9,10</sup> The general formula of the products was proposed to be  $(LiX_x)_y \cdot 2Al(OH)_3 \cdot nH_2O$ , where  $n$  is the number of waters of hydration,  $y$  is the number of lithium atoms present for each 2 mol of aluminum, and  $x$  is the reciprocal of the valence of the anion. The value for  $y$  was reported in the range  $0.5 \leq y \leq 1.2$ .

(1) Allen, E. T.; Rogers, H. F. *Am. Chem. J.* **1900**, *24*, 304.  
 (2) Prociw, D. *Collect. Czech. Chem. Commun.* **1929**, *1*, 95.  
 (3) Horan, H.; Damiano, J. B. *J. Am. Ceram. Soc.* **1935**, *57*, 2434.  
 (4) Lileev, I. S.; Sachenko-Sakun, L. K.; Guseva, I. V. *Russ. J. Inorg. Chem.* **1968**, *13*(2), 213.  
 (5) Frenkel, M.; Glasner, A.; Sarig, S. *J. Phys. Chem.* **1980**, *84*, 507.  
 (6) Van Straten, H. A.; Schoonen, M. A. A.; De Bruyn, P. L. *J. Colloid, Interface Sci.* **1985**, *103*, 493.

(7) Gorin, P.; Marchon, J.-C.; Tranchant, J.; Kovacevic, S.; Marsault, J.-P. *Bull. Soc. Chim. Fr.* **1970**, 3790.  
 (8) Serna, C. J.; Rendon, J. L.; Iglesias, J. E. *Clays Clay Miner.* **1982**, *30*, 180.  
 (9) Bauman, W. C.; Lee, J. M.; Burba, J. L. U.S. Patent 4 348 296, 1982.  
 (10) Bauman, W. C.; Lee, J. M. U.S. Patent 4 348 297, 1982.

In this paper we address the general question, can the framework of aluminum trihydroxide imbibe lithium salts and, if so, what compositions result, and perhaps most important, can we develop synthetic procedures to simplify the preparation of pure lithium dialuminate?

### Experimental Section

**Syntheses. Preparation of Bayerite.** Crystalline bayerite,  $\text{Al}(\text{OH})_3$ , was prepared by precipitating  $\text{Al}^{3+}(\text{aq})$  with 30 wt % ammonia solution, followed by recrystallization using an excess of ammonia. For example, 9.1 mL of 30 wt %  $\text{NH}_3(\text{aq})$  was slowly added with stirring to 150 mL of 0.28 M  $\text{Al}^{3+}(\text{aq})$  solution, followed by addition of 81 mL of ammonia solution and 83 mL of water. The  $\text{Al}^{3+}(\text{aq})$  solution was prepared from  $\text{AlCl}_3 \cdot 6\text{H}_2\text{O}$ . After the first addition of ammonia the pH of the solution was about 7. In order to cause recrystallization, and inasmuch as  $\text{Al}(\text{OH})_3$  is essentially insoluble over the pH range 4–10, additional base was necessary to increase the pH to about 11 where  $\text{Al}(\text{OH})_3$  is slightly soluble.

The solution was left unstirred at room temperature for 12 h. The solution was decanted and the crystalline product washed several times with 150 mL of distilled water until no trace of chloride ion in the wash water could be detected with silver nitrate. The solid was dried at 95 °C in a circulating-air oven. Powder X-ray diffraction (XRD) showed the expected<sup>11</sup> diffraction pattern of bayerite. On the basis of thermogravimetric analysis (TGA), the  $\text{Al}(\text{OH})_3$  was found to lose 34.46% by weight upon heating to 950 °C compared with an expected weight loss of 34.64%.

**Preparation of  $[\text{LiAl}_2(\text{OH})_6]^+\text{OH}^- \cdot 2\text{H}_2\text{O}$ . Method A.** This method used freshly precipitated, unseparated bayerite to which LiOH solution was added.<sup>9</sup> For example, 8.9 mL of 30 wt %  $\text{NH}_3(\text{aq})$  solution was added to 200 mL of 0.21 M  $\text{Al}^{3+}(\text{aq})$  to give a pH of 7. While the mixture was stirred, 50 mL of 3.31 M lithium hydroxide solution was added slowly. The mixture was heated at 95 °C for 4 h and then kept at room temperature for 12–15 h. The solid, crystalline product was washed with distilled water until the wash water was free of chloride ion as indicated by the  $\text{AgNO}_3$  test. The precipitate was then dried under vacuum at room temperature. Drying at higher temperature was avoided because the loosely bound waters of hydration are easily lost at or near 100 °C.

The XRD pattern of the vacuum-dried product resembled that reported<sup>7</sup> for the dialuminate. However, close inspection revealed the characteristic peak of bayerite at  $2\theta = 18.6^\circ$  (Cu  $K\alpha$  radiation). This may be due to unreacted  $\text{Al}(\text{OH})_3$  but is more likely the result of LiOH leaching in the washing step, or some combination. In addition, two very broad peaks were observed in the powder pattern at about 40.0 and 47.5° (Cu  $K\alpha$  radiation) that can be attributed to a mixed-anion composition  $[\text{LiAl}_2(\text{OH})_6]^+\text{OH}^{1-x}\text{Cl}^{x-} \cdot 2\text{H}_2\text{O}$  ( $0 \leq x \leq 1$ ). Incorporation of chloride ion results when the freshly precipitated  $\text{Al}(\text{OH})_3$  is not separated from the solution that contains chloride ion prior to the addition of the lithium salt. This effect can be demonstrated quite clearly with the end members  $[\text{LiAl}_2(\text{OH})_6]^+\text{Cl}^- \cdot n\text{H}_2\text{O}$  ( $n \approx 0.5$ ) and  $[\text{LiAl}_2(\text{OH})_6]^+\text{OH}^- \cdot 2\text{H}_2\text{O}$ . The majority of the diffraction peaks in their diffraction patterns are superimposable except those that fall in the region  $2\theta = 40\text{--}50^\circ$ , which results in the observed broadened diffraction pattern. This same broadening effect has been observed<sup>8</sup> in the carbonate  $[\text{LiAl}_2(\text{OH})_6]_2^+\text{CO}_3^{2-} \cdot n\text{H}_2\text{O}$  ( $n \approx 0.5$ ) due to partial incorporation of  $\text{Cl}^-$  and  $\text{OH}^-$ . This method is not satisfactory for the preparation of a pure compound without separating the  $\text{Al}(\text{OH})_3$  from solutions that contain exchangeable anions.

**Method B.** The problems encountered in method A were largely overcome by first preparing polycrystalline bayerite free of any  $\text{NH}_4\text{Cl}$  and then reacting it with LiOH solution. A large excess of water is not required for reaction. To prepare  $[\text{LiAl}_2(\text{OH})_6]^+\text{OH}^- \cdot 2\text{H}_2\text{O}$  by what is essentially an incipient wetness procedure, a weighted amount of  $\text{Al}(\text{OH})_3$  was contacted with a stoichiometric amount of LiOH and sufficient water to slurry the sample. In a typical reaction, 1 g of dried  $\text{Al}(\text{OH})_3$  was added to 2 mL of 3.21 M LiOH ( $\text{LiOH} \cdot \text{H}_2\text{O}$ , Alfa Products) solution. The mixture was kept at room temperature, vacuum-dried daily, ground in a mortar and pestle, and then reslurried with 2 mL of water. Because of the particle size effect, the reaction took 3 days to go to completion.

**Method C.** There are several potential problems with method B. The water that is in excess can dissolve some of the alumina, which then must reprecipitate upon drying as  $[\text{LiAl}_2(\text{OH})_6]^+\text{OH}^- \cdot 2\text{H}_2\text{O}$  or some other detrital compound. Secondly, carbon dioxide from the air can react to form carbonate, which in turn can exchange with hydroxide ion to form traces of a mixed-anion dialuminate. These problems, although appar-

**Table I.** Observed and Calculated X-ray Diffraction Data

$d_{\text{obsd}}/\text{\AA}$	$d_{\text{calcd}}/\text{\AA}$	$hkl$	$I_{\text{obsd}}$
11.3	11.337	002	<5
7.563	7.559	003	100
4.418	4.419	100	35
$\approx 4.33$	4.338	101	
$\approx 4.11$	4.118	102	
3.778	3.815	103	63
	3.779	006	
2.834	2.872	106	<1
	2.834	008	
2.536	2.552	110	64
	2.535	111	
2.491	2.519	009	
	2.489	112	
2.225	2.224	115	27
	2.210	200	
	2.199	201	
1.895	1.908	206	37
	1.896	118	
	1.889	0,0,12	
1.694	1.695	1,1,10	5
1.604	1.603	1,1,11	4
	1.602	214	
1.473	1.473	300	17
	1.470	301	
1.447	1.446	303	19
	1.440	1,1,13	
	1.439	218	
	1.436	2,0,12	
	1.430	1,0,15	
	1.417	0,0,16	
1.372	1.373	306	6
	1.369	2,0,13	
	1.367	1,1,14	
1.267	1.277	1,0,17	1
	1.276	220	
	1.274	221	
	1.272	309	
	1.268	222	
	1.260	0,0,18	
	1.258	223	
1.235	1.239	1,1,16	2
	1.235	3,0,10	
1.228	1.228	225	2
	1.226	310	
	1.224	311	

ently not major problems in method B, can be avoided by the direct reaction of  $\text{LiOH} \cdot \text{H}_2\text{O}$  with polycrystalline  $\text{Al}(\text{OH})_3$ . These solids when placed together and exposed to water vapor react. The dialuminate forms in 2–3 days at room temperature. For example, 0.5 g ( $6.4 \times 10^{-3}$  mol) of dried  $\text{Al}(\text{OH})_3$  and 0.1348 g ( $3.2 \times 10^{-3}$  mol) of  $\text{LiOH} \cdot \text{H}_2\text{O}$  were mixed by grinding in a mortar. The mixture was placed in a glass flow reactor at room temperature and purged with water-saturated nitrogen gas. For the reaction to go to completion the sample was ground at several intervals. The advantage of this method, compared with method B, is that formation of carbonates and detrital compounds formed by dissolution and reprecipitation are avoided.

**Characterization. X-ray Diffraction (XRD).** Powder diffraction patterns were recorded with Cu  $K\alpha$  radiation ( $\lambda = 1.5418 \text{\AA}$ ) and a Ni filter on a Rigaku diffractometer. Data were collected by step scanning over the angular range  $5^\circ \leq 2\theta \leq 80^\circ$  in increments of  $0.02^\circ 2\theta$  at room temperature, and intensities were measured by peak integration.

Figure 1 shows the diffraction pattern of the  $[\text{LiAl}_2(\text{OH})_6]^+\text{OH}^- \cdot 2\text{H}_2\text{O}$  prepared by method C. Hexagonal unit cell parameters,  $a = 5.103(1) \text{\AA}$  and  $c = 22.674(8) \text{\AA}$ , were calculated by using the programs TREOR and POLSQ.<sup>12</sup> The small vertical lines below the diffraction

(11) No. 20-11, Joint Committee on Powder Diffraction Standards, Swarthmore, PA.

(12) Werner, P. E. TREOR, FORTRAN program, University of Stockholm, 1984. Keszlér, D.; Ibers, J. POLSQ, FORTRAN program, Northwestern University, 1983.

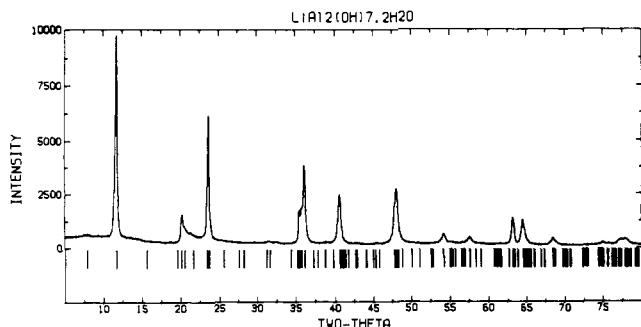


Figure 1. Powder X-ray diffraction pattern of  $[\text{LiAl}_2(\text{OH})_6]^+\text{OH}\cdot 2\text{H}_2\text{O}$ .

pattern in Figure 1 indicate the calculated position of all possible Bragg reflections. Table I lists the observed ( $d_{\text{obsd}}/\text{\AA}$ ) and calculated ( $d_{\text{calcd}}/\text{\AA}$ ) positions, their Miller indices ( $hkl$ ), and relative intensities ( $I_{\text{obsd}}$ ). Omitted from Table I were the unobserved reflections. In the range  $6^\circ \leq 2\theta \leq 40^\circ$  ( $14.73 \leq d/\text{\AA} \leq 2.254$ ) the unobserved reflections were as follows for  $d/\text{\AA}$ , ( $hkl$  unobsd): 5.669, (004); 4.535, (005); 3.485, (104); 3.239, (007); 3.165, (105); 2.613, (107); 2.417, (113); 2.386, (108); 2.327, (114); 2.267, (0,0,10).

**Thermogravimetric Analysis (TGA).** Thermogravimetric measurements were made with a Du Pont 9900 thermal analysis system. All thermograms were run at a heating rate of  $10^\circ/\text{min}$  under flowing dry air at  $50 \text{ cm}^3/\text{min}$ .

**Infrared (IR).** Infrared spectra were collected on a Perkin-Elmer Model 283 spectrophotometer in KBr and CsI pellets.

**Atomic Absorption (AA).** A Hitachi atomic absorption spectrometer was used to analyze for soluble lithium and aluminum remaining in solution after product had formed (method A).

## Results and Discussion

The reported syntheses of  $[\text{LiAl}_2(\text{OH})_6]^+\text{OH}\cdot 2\text{H}_2\text{O}$  and related compounds<sup>13</sup> use an excess of the lithium salt to precipitate the insoluble lithium dialuminate. Some unreacted aluminum trihydroxide can be expected to form in less concentrated salt solution or during washing with water to remove excess salts. We find, for example, that when solid  $[\text{LiAl}_2(\text{OH})_6]^+\text{OH}\cdot 2\text{H}_2\text{O}$  is contacted with 0.48 M lithium hydroxide solution at room temperature ( $21^\circ\text{C}$ ), the  $\text{Li}^+$  ion concentration increases to 0.51 M and the  $\text{Al}^{3+}$  ion concentration to about 0.06 M, suggesting a congruent dissolution process under these conditions. At lower initial  $\text{Li}^+$  ion concentrations a separate solid phase of  $\text{Al}(\text{OH})_3$  (bayerite) can be identified, suggesting an additional incongruent dissolution-precipitation process. At higher initial  $\text{Li}^+$  ion concentrations only  $[\text{LiAl}_2(\text{OH})_6]^+\text{OH}\cdot 2\text{H}_2\text{O}$  was obtained. These observations are in accord with others<sup>3</sup> that showed that the composition of the insoluble lithium aluminate remained the same over a range in pH and lithium ion concentration.

In method B we have developed an incipient wetness method of synthesis. This procedure ensures that the total amount of soluble lithium and aluminum species is reduced to a minimum due to the limited volume of free water. The desired product  $[\text{LiAl}_2(\text{OH})_6]^+\text{OH}\cdot 2\text{H}_2\text{O}$  forms even though the total molar Li/Al ratio approaches that found in the solid phase, Li/Al = 0.5. The reaction occurs at room temperature, probably almost entirely through imbibition of LiOH and water into the solid  $\text{Al}(\text{OH})_3$  framework, although some fraction may form through dissolution and reprecipitation. Because the total molar Li/Al ratio is 0.5 in method B, and the concentration of soluble lithium is greater than that of alumina, there should also be some small amounts of unreacted  $\text{Al}(\text{OH})_3$  present. We could not detect it by XRD. The small amount of lithium and aluminum present as soluble species in the incipient wetness technique prior to vacuum-drying may react upon drying with the trace of unreacted bayerite or form some unnoticed precipitate.

In method C the monohydrate  $\text{LiOH}\cdot\text{H}_2\text{O}$  was ground with aluminum trihydroxide to form a simple mixture. In dry air and at room temperature no reaction was observed to occur. In air ( $\text{CO}_2$  free) or nitrogen saturated with water vapor, again at room

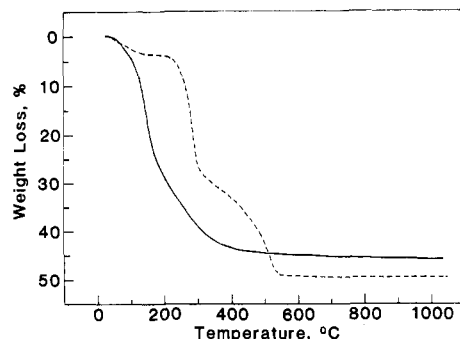


Figure 2. Thermogravimetric behavior of (a)  $[\text{LiAl}_2(\text{OH})_6]^+\text{OH}\cdot 2\text{H}_2\text{O}$  (solid curve) and (b)  $[\text{LiAl}_2(\text{OH})_6]^+\text{NO}_3^-\cdot 0.5\text{H}_2\text{O}$  (dashed curve).

temperature, the solids were found to react with the uptake of an additional 1 mol of water/mol of  $\text{LiOH}\cdot\text{H}_2\text{O}$  to form the compound  $[\text{LiAl}_2(\text{OH})_6]^+\text{OH}\cdot 2\text{H}_2\text{O}$ . Some additional water, 14 wt. %, is absorbed on the solid. This water can be removed by vacuum-drying. This water is presumably involved in surface and pore filling, and may assist in surface and interparticle diffusion of lithium hydroxide. Recrystallization of the dialuminate on surfaces and inside pores due to soluble aluminum species would not occur to a significant extent because of the limited volume of excess water.

X-ray diffraction and thermogravimetric analysis have been used to characterize the  $[\text{LiAl}_2(\text{OH})_6]^+\text{OH}\cdot 2\text{H}_2\text{O}$  prepared by these three different methods. Figure 1 shows a typical X-ray diffraction pattern of the product from method B or C when the reaction is complete. The reported<sup>14</sup> powder X-ray diffraction pattern of lithium dialuminate matches the diffraction pattern prepared by salt imbibition. The presence of unreacted  $\text{Al}(\text{OH})_3$  can be detected by the strongest diffraction peak in the pattern reported<sup>11</sup> for bayerite, the (001) X-ray reflection, which occurs at  $2\theta = 18.65^\circ$  ( $\text{Cu K}\alpha$  radiation). Unreacted bayerite could be detected by XRD in samples prepared by method A, but not by methods B and C. Thermogravimetric analysis of the product from methods A, B, and C gave weight losses of 43.64, 46.38, and 45.98% respectively, compared with an expected 45.83% weight change. This compares with a 47.35% loss in earlier preparations by direct precipitation.<sup>4</sup> Figure 2a is a TGA trace of the sample prepared by method C. On the basis of the combined XRD and TGA results, it appears that an essentially quantitative yield of lithium dialuminate can be obtained by the imbibition of lithium hydroxide and water into particles of aluminum trihydroxide by methods B and C.

Previous work on hydroxalite-type compounds<sup>13</sup> has shown that their structures consist of positively charged double-hydroxide sheets and intermediate layers formed from anions and water molecules. A variety of synthetic aluminum-lithium double hydroxides,  $[\text{LiAl}_2(\text{OH})_6]^+\text{X}^{m-}_{1/m}\cdot n\text{H}_2\text{O}$ , have been made,<sup>15</sup> where  $\text{X}^{m-}$  is an interlayer anion found in the intermediate layer that balances the positive charge on the double-hydroxide sheet. In contrast, the structure of bayerite<sup>16</sup> has a pseudo-trigonal layer structure, in which the oxygen atoms approximate hexagonal closest packing of spheres. The aluminum-centered antiprisms are distorted so the O-O distances are shorter for the triangular faces (2.61–3.00 Å) and shared edges (2.92–3.01 Å) than for edges facing empty sites (3.16–3.24 Å). These sheets are similar to those found in gibbsite. The difference between bayerite and gibbsite, in a structural sense, is found in the sequence of the hydroxide layers. In gibbsite<sup>17,18</sup> the hydroxide layers are sequenced  $-\text{AB}-\text{BA}-\text{AB}-$  whereas in bayerite they are  $-\text{AB}-\text{AB}-\text{AB}-$ . Both bayerite and gibbsite<sup>19</sup> react with lithium salts to form hydro-

(13) Miyata, S. *Clays Clay Miner.* **1975**, *23*, 369.

(14) No. 31-704, Joint Committee on Powder Diffraction Standards, Swarthmore, PA.

(15) Ulibarri, M. A.; Hernandez, M. J.; Cornejo, J.; Serna, C. J. *Mater. Chem. Phys.* **1986**, *14*, 569.

(16) Rothbauer, R.; Zigan, F.; O'Daniel, H. Z. *Kristallogr.* **1967**, *125*, 317.

(17) Megaw, H. D. Z. *Kristallogr.* **1934**, *87*, 185.

(18) Saalfeld, H.; Wedde, M. Z. *Kristallogr.* **1974**, *139*, 129.

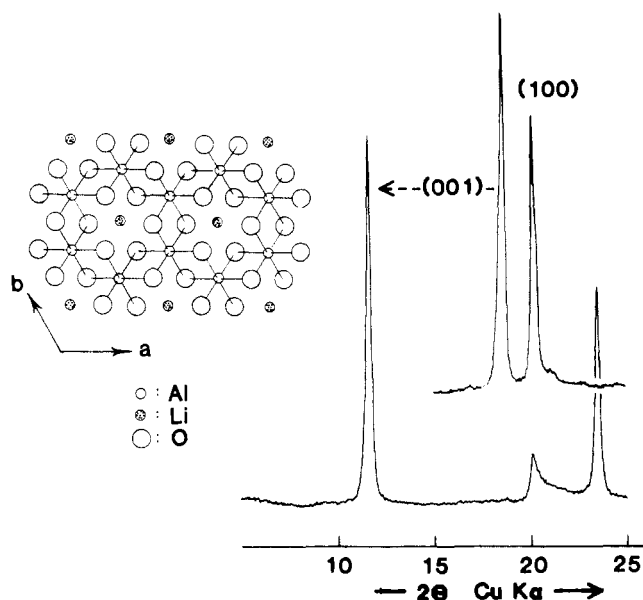


Figure 3. Shift in the (001) X-ray reflection to larger  $d$  spacing (right) and presumed basal plane  $[\text{LiAl}_2(\text{OH})_6]^+$  (left) of monoclinic bayerite after reaction with lithium hydroxide and water.

talcite-like double-hydroxide layers  $[\text{LiAl}_2(\text{OH})_6]^+$ . To balance the positive charge and, we speculate, to form another essentially close-packed intermediate layer of oxygen atoms, one hydroxide anion and two water molecules are incorporated into the structure. Presumably, a complex system of hydrogen bonds is also generated.

Serna et al.<sup>8</sup> have shown with selected area electron diffraction that the  $[\text{LiAl}_2(\text{OH})_6]^+$  sheets retain hexagonal symmetry. The X-ray diffraction pattern of  $[\text{LiAl}_2(\text{OH})_6]^+\text{OH}^- \cdot 2\text{H}_2\text{O}$  prepared by method C has been indexed with hexagonal unit cell parameters,  $a = 5.103$  (1) Å and  $c = 22.674$  (8) Å. The tripling of the  $c$  axis is indicated by the observed reflections with  $l \neq 3n$ ; 101, 102, 111, 115, etc. The oxygen atoms probably approximate closest packing with three three-layer sheets of about 7.6-Å thickness that form a nine-layer (9L) structure. The large number of 9L polytypes, and sequences other than 9L that are possible, make the interpretation of the intensities observed in Figure 1 difficult. Single crystals, perhaps grown by hydrothermal techniques, would be desirable.

Figure 3 depicts the qualitative relationship just described between bayerite and lithium dialuminate. The lattice constants of the monoclinic cell<sup>16</sup> of bayerite can be transformed with the transformation matrix

$$\begin{bmatrix} 1 & 0 & 0 \\ -1/2 & 1/2 & 0 \\ 0 & 0 & 1 \end{bmatrix}$$

to a pseudohexagonal setting with  $a = 5.1$  Å and  $c = 4.7$  Å, and then compared with the approximate hexagonal cell  $a = 5.1$  Å and  $c/3 = 7.5$  Å reported<sup>14</sup> for the dialuminate. The (001) X-ray reflection of  $[\text{LiAl}_2(\text{OH})_6]^+\text{OH}^- \cdot 2\text{H}_2\text{O}$  is shifted to a lower angle because of the additional layer of hydroxide ions and water molecules relative to the bayerite structure (see Figure 3).

Similarly, the hexagonal cell of  $[\text{LiAl}_2(\text{OH})_6]^+\text{OH}^- \cdot 2\text{H}_2\text{O}$  can be transformed to a monoclinic cell by the transformation matrix

$$\begin{bmatrix} 1 & 0 & 0 \\ 1 & 2 & 0 \\ 0 & 0 & 1 \end{bmatrix}$$

and the diffraction pattern satisfactorily reindexed with the new cell parameters  $a = 5.099$  (6) Å,  $b = 8.89$  (1) Å,  $c = 22.64$  (2) Å ( $c/3 = 7.55$  Å), and  $\beta = 90.4$  (1)°. The monoclinic cell is, as it should be, very similar to the bayerite monoclinic unit cell,<sup>16</sup>

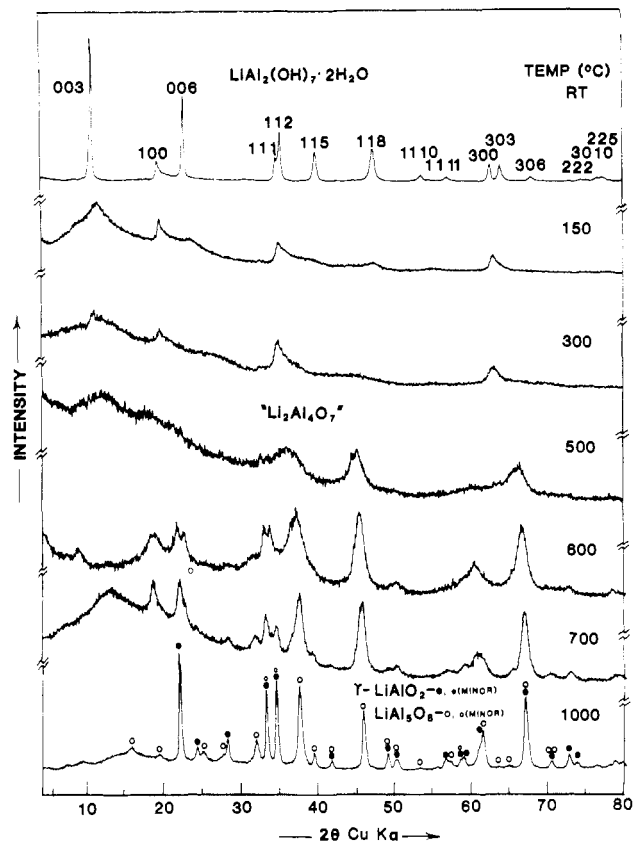


Figure 4. Powder X-ray diffraction patterns after calcination of  $[\text{LiAl}_2(\text{OH})_6]^+\text{OH}^- \cdot 2\text{H}_2\text{O}$  from 100 to 1000 °C.

where  $a = 5.068$  (2) Å,  $b = 8.703$  (4) Å,  $c = 4.737$  (3) Å, and  $\beta = 90.27$  (5)°. Again we see that the essential difference is the increase in the  $c$  dimension of 2.81 Å, about that expected for an additional layer of hydroxide ions and water molecules.

Using the incipient wetness techniques described in methods B and C, it was possible to prepare the lithium dialuminate compounds  $[\text{LiAl}_2(\text{OH})_6]^+\text{X}^- \cdot n\text{H}_2\text{O}$  where  $\text{X} = \text{Cl}^-$ ,  $\text{Br}^-$ ,  $\text{I}^-$ , and  $\text{NO}_3^-$ . At constant temperature and water vapor pressure, the amount of water incorporated,  $n$ , was found to vary and depend on the anion. For example, we have prepared  $[\text{LiAl}_2(\text{OH})_6]^+\text{Cl}^- \cdot n\text{H}_2\text{O}$  ( $n \approx 0.5$ ) using  $\text{LiCl}$  and method C. This homoanionic compound has proven useful in explaining the observations made earlier concerning the two broad X-ray reflections (115) and (118) at  $2\theta \approx 40$  and  $47^\circ$ , respectively, in the sample prepared by method A. The chloride and hydroxide compounds are presumably isostructural. The lithium dialuminate prepared in method A is evidently a mixture, or solid solution of the two compounds, which gives rise to the peak broadening we have observed, and may account for the reported<sup>14</sup> large relative intensities of these reflections. The mixed-anionic nature of the compound evidently results from using aluminum trichloride and the fact<sup>9,10,13</sup> that these compounds are known anion exchangers. Methods B and C avoid anion interdiffusion and heteroanionic compositions. To eliminate anion interdiffusion in method A would require that all soluble salts be removed from solution prior to the addition of the lithium hydroxide solution and formation of the dialuminate compound.

Layered inorganic anion exchangers are of interest<sup>20</sup> for selective sorption of weak acids, selective anion exchange, and other properties related to their unique structure. These compounds may also serve as potential precursors to interesting new mixed-metal oxides upon dehydration and dehydroxylation.

In Figure 4 we show the X-ray powder diffraction patterns that result after calcining  $[\text{LiAl}_2(\text{OH})_6]^+\text{OH}^- \cdot 2\text{H}_2\text{O}$  at fixed tem-

(19) Nemudry, A. P.; Isupov, V. P.; Kotsupalo, N. P.; Boldyrev, V. V. *React. Solids* 1986, 1, 221.

(20) Sissoko, I.; Iyagba, E. T.; Sahai, R.; Biloen, P. J. *Solid State Chem.* 1985, 41, 88.

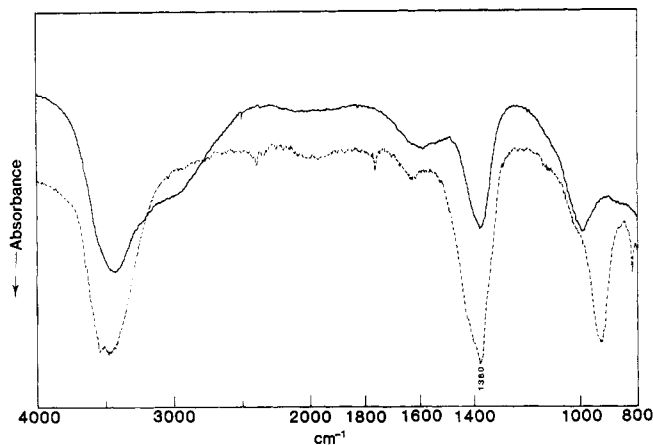


Figure 5. Infrared spectra (800–4000  $\text{cm}^{-1}$ ) of  $[\text{LiAl}_2(\text{OH})_6]^+\text{X}^{m-}/_m n\text{H}_2\text{O}$ .  $\text{X}^{m-}$ :  $\text{OH}^-$  (solid line);  $\text{NO}_3^-$  (dashed line).

peratures from 100 to 1000 °C. The powder X-ray diffraction pattern of  $[\text{LiAl}_2(\text{OH})_6]^+\text{OH}^- \cdot 2\text{H}_2\text{O}$  prepared by method C is shown at the top of Figure 4 with the appropriate Miller indices indicated (see Table I). The diffraction patterns that follow in Figure 4 were obtained by sequentially heating in air the same sample to the temperature indicated and maintaining that temperature for 30 minutes, followed by cooling to room temperature and reexamination by XRD.

There is no temperature where a totally featureless diffraction pattern was observed. Below 150 °C significant changes have occurred in the precursor as demonstrated by thermogravimetric analysis, which shows a weight loss of about 15% up to 150 °C (see Figure 2). The X-ray diffraction patterns at 150 and 300 °C are consistent with the gravimetric observation and show that the initial dehydration and dehydroxylation processes have overlapped and by 150 °C produce a solid with only remnant order. Above 300 and by 500 °C new features begin to appear in the diffraction pattern that indicate the onset and nucleation of a poorly crystalline transitional phase. This material has a specific surface area of about 130  $\text{m}^2/\text{g}$  and pore volume of 0.23  $\text{cm}^3/\text{g}$  as determined by the BET method. At 600 °C there is clear indication that  $\gamma\text{-LiAlO}_2$  and  $\text{LiAl}_2\text{O}_6$ <sup>21</sup> have begun to crystallize, and by 1000 °C the process is complete and there is a 3/1 molar mixture of the two compounds. The XRD and TGA results demonstrate that no significant loss of lithium oxide occurs during the calcination process.

The translational stage that occurs in the approximate temperature range 400–900 °C has been studied in more detail. One factor that increases the amount of the transitional lithiated alumina " $\text{Li}_2\text{Al}_4\text{O}_7$ " (see below) and suppresses the formation of  $\gamma\text{-LiAlO}_2$  and  $\text{LiAl}_2\text{O}_6$  in this temperature range is the presence of chloride ion in the hydroxide precursor. This may result from the substitution of oxide ion by chloride ion in the transitional framework, i.e.  $\text{Li}_2\text{Al}_4\text{O}_6\text{Cl}_2$ , and is under further investigation. There is considerable general interest<sup>22</sup> in the preparation, structure, and mechanism of incorporation of other metal atoms into the transitional alumina structures.

The nitrate  $[\text{LiAl}_2(\text{OH})_6]^+\text{NO}_3^- \cdot 0.5\text{H}_2\text{O}$  was prepared by method C. Structural similarities of the nitrate and hydroxide are evident from their infrared (IR) spectra shown in Figures 5 (800–4000  $\text{cm}^{-1}$ ) and 6 (200–800  $\text{cm}^{-1}$ ). Both spectra have similar absorption maxima due to water and hydroxyl groups, and in addition the absorption band of  $\text{NO}_3^-$  ion intensifies the absorption at around 1380  $\text{cm}^{-1}$ . Regions characteristic of  $\text{AlO}_6$  octahedra (370–750  $\text{cm}^{-1}$ ) and  $\text{LiO}_6$  vibrations (200–350  $\text{cm}^{-1}$ ) are similar to those reported<sup>8,23</sup> previously. In contrast to the hydroxide precursor, the nitrate compound decomposes in air in definite

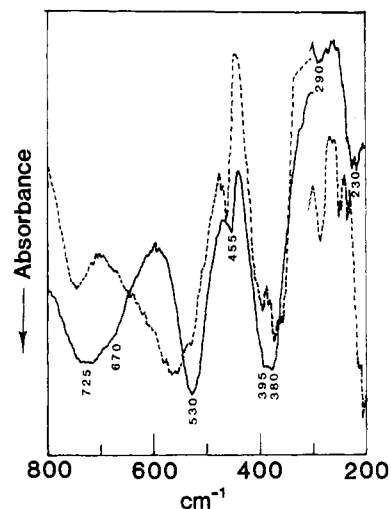


Figure 6. Infrared spectra (200–800  $\text{cm}^{-1}$ ) of  $[\text{LiAl}_2(\text{OH})_6]^+\text{X}^{m-}/_m n\text{H}_2\text{O}$ .  $\text{X}^{m-}$ :  $\text{OH}^-$  (solid line);  $\text{NO}_3^-$  (dashed line).

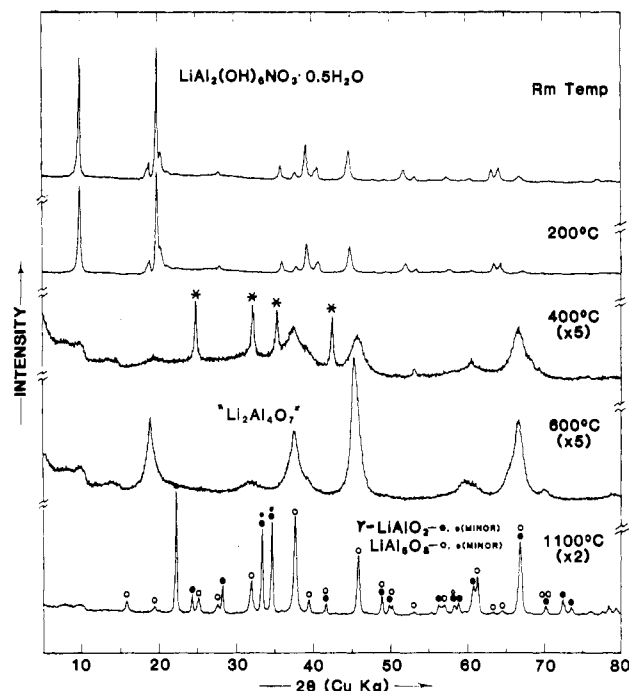


Figure 7. Powder X-ray diffraction patterns after calcination of  $[\text{LiAl}_2(\text{OH})_6]^+\text{NO}_3^- \cdot 0.5\text{H}_2\text{O}$  from 200 to 1100 °C.

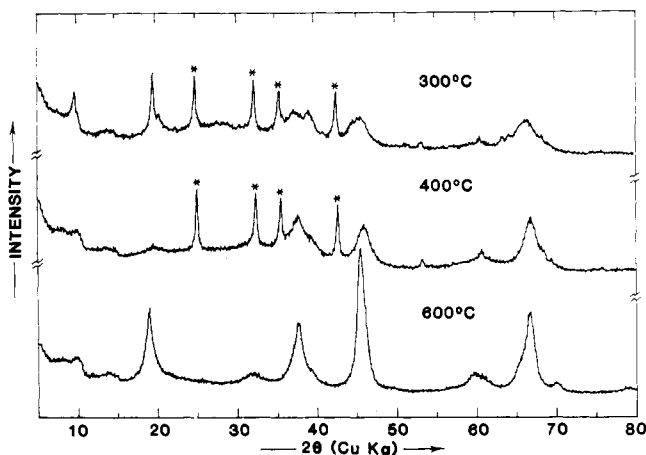


Figure 8. Powder X-ray diffraction patterns after calcination of  $[\text{LiAl}_2(\text{OH})_6]^+\text{NO}_3^- \cdot 0.5\text{H}_2\text{O}$  from 300 to 600 °C. The diffraction peaks caused by  $\text{LiNO}_3$  are marked with an asterisk.

(21) Hummel, F. A.; Sastry, B. S. R.; Wotring, D. *J. Am. Ceram. Soc.* **1958**, *41*, 88.

(22) Pugar, E. A.; Morgan, P. E. D. *J. Am. Ceram. Soc.* **1986**, *69*, C-120.

(23) Hernandez, M. J.; Ulibarri, M. A.; Rendon, J. L.; Serna, C. *J. Phys. Chem. Miner.* **1985**, *12*, 34.

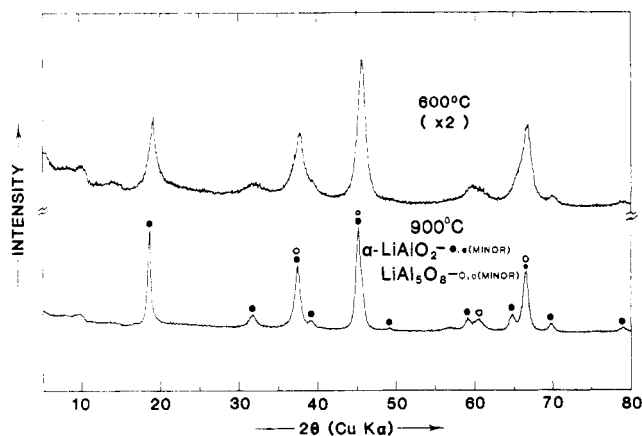


Figure 9. Powder X-ray diffraction pattern of  $[\text{LiAl}_2(\text{OH})_6]^+\text{NO}_3^- \cdot 0.5\text{H}_2\text{O}$  after calcination at 600 and 900 °C. The diffraction peaks of  $\alpha\text{-LiAlO}_2$  (●) and  $\text{LiAl}_5\text{O}_8$  (○) are shown for the 900 °C sample.

stages as a function of temperature. Figure 2b illustrates the decomposition behavior of the nitrate compound as followed by thermogravimetric analysis.

Figure 7 illustrates powder X-ray diffraction patterns, recorded at ambient conditions, of the nitrate compound as prepared, and after calcination at 200, 400, 600, and 1100 °C. From the first stage of decomposition the thermal behavior of the nitrate is unlike

that of the hydroxide, in that the nitrate can be dehydrated without significant structural changes. Upon further heating there is clear evidence for lithium nitrate and a poorly crystalline compound, perhaps an alumina. From Figure 8 we observe in more detail that at 300 °C the precursor is a mixture of dehydrated starting material, lithium nitrate, and a poorly crystalline spinel-like phase. After 400 °C was reached, the starting material has disappeared. By 600 °C the nitrate has decomposed and the mixture has reacted to form a mixture of  $\alpha\text{-LiAlO}_2$  and  $\text{LiAl}_5\text{O}_8$  (3/1 molar ratio), which is stable up to 900 °C (see Figure 9). By 1100 °C  $\alpha\text{-LiAlO}_2$  has converted to  $\gamma\text{-LiAlO}_2$  to form a mixture of  $\gamma\text{-LiAlO}_2$  and  $\text{LiAl}_5\text{O}_8$ , the known compounds stable at high temperature in this region of the  $\text{Li}_2\text{O}-\text{Al}_2\text{O}_3$  system.<sup>21</sup> Evidently, if a compound such as  $\text{Li}_2\text{Al}_4\text{O}_7$  can be formed from the decomposition of  $[\text{LiAl}_2(\text{OH})_6]^+\text{OH}^- \cdot 2\text{H}_2\text{O}$ , it will be unstable with respect to a mixture of  $\alpha\text{-LiAlO}_2$  and  $\text{LiAl}_5\text{O}_8$  at intermediate temperatures and to the  $\gamma$ -form of  $\text{LiAlO}_2$  at elevated temperature.

**Acknowledgment.** We thank the National Science Foundation and Northwestern Materials Research Center (Grant DMR 8520280) and Alcoa Foundation for their support of this research. K.R.P. thanks Du Pont for a Young Faculty Award.

**Registry No.**  $\text{Al}(\text{OH})_3$ , 21645-51-2;  $\text{AlCl}_3$ , 7446-70-0;  $\text{NH}_4\text{OH}$ , 1336-21-6;  $\text{LiOH}$ , 1310-65-2;  $[\text{LiAl}_2(\text{OH})_6]^+\text{OH}^- \cdot 2\text{H}_2\text{O}$ , 12344-53-5;  $[\text{LiAl}_2(\text{OH})_6]^+\text{Cl}^- \cdot n\text{H}_2\text{O}$  ( $n = 0.5$ ), 110027-58-2;  $\text{LiOH} \cdot \text{H}_2\text{O}$ , 1310-66-3;  $\text{LiCl}$ , 7447-41-8;  $\text{LiAlO}_2$ , 12003-67-7;  $\text{LiAl}_5\text{O}_8$ , 12005-14-0;  $\text{Li}_2\text{Al}_4\text{O}_7$ , 12446-24-1;  $[\text{LiAl}_2(\text{OH})_6]^+\text{NO}_3^- \cdot 0.5\text{H}_2\text{O}$ , 110027-60-6;  $\text{LiNO}_3$ , 7790-69-4.

Contribution from the Lehrstuhl für Anorganische Chemie I, Ruhr-Universität, D-4630 Bochum, FRG, and Anorganisch Chemisches Institut der Universität, D-6900 Heidelberg, FRG

## General Route to $\mu$ -Hydroxo-Bis( $\mu$ -acetato)-Bridged Heterometal Dinuclear Complexes. Syntheses, Magnetic and Redox Properties, Electronic Spectra, and Molecular Structures of the Cr(III)-Co(II) and Cr(III)-Fe(II) Species

Phalguni Chaudhuri,\*† Manuela Winter,† Heinz-Josef Küppers,† Karl Wieghardt,† Bernhard Nuber,† and Johannes Weiss†

Received March 19, 1987

A series of heterodinuclear complexes of general formula  $[\text{LCr}(\mu\text{-OH})(\mu\text{-CH}_3\text{COO})_2\text{ML}](\text{ClO}_4)_2$  ( $\text{L} = \text{C}_9\text{H}_{21}\text{N}_3$ , 1,4,7-trimethyl-1,4,7-triazacyclononane;  $\text{M} = \text{Zn}(\text{II}), \text{Cu}(\text{II}), \text{Ni}(\text{II}), \text{Co}(\text{II}), \text{Fe}(\text{II}),$  and  $\text{Mn}(\text{II})$ ) have been synthesized. The homodinuclear complex  $[\text{LCr}(\mu\text{-OH})(\mu\text{-CH}_3\text{COO})_2\text{CrL}](\text{ClO}_4)_3$  has also been isolated. The crystal molecular structures of the Cr(III)-Fe(II) and Cr(III)-Co(II) complexes have been established by X-ray diffraction methods. Both of them crystallize in the triclinic system, space group  $C_1^1\text{-P}\bar{1}$ , with lattice constants  $a = 12.637$  (4) Å,  $b = 16.254$  (5) Å,  $c = 19.141$  (7) Å,  $\alpha = 84.68$  (3)°,  $\beta = 73.92$  (3)°,  $\gamma = 68.33$  (2)°, and  $Z = 4$  for the Cr(III)-Fe(II) species and  $a = 12.535$  (4) Å,  $b = 16.263$  (6) Å,  $c = 19.111$  (8) Å,  $\alpha = 84.66$  (3)°,  $\beta = 74.27$  (3)°,  $\gamma = 68.59$  (3)°, and  $Z = 4$  for the Cr(III)-Co(II) complex. Least-squares refinement of the structures led to a final  $R$  value of 0.087 for 5285 unique reflections and 0.083 for 8999 unique reflections in the case of the Cr(III)-Fe(II) and Cr(III)-Co(II) complexes, respectively. The structures consist of heteroatom binuclear cations  $[\text{LCr}(\mu\text{-OH})(\mu\text{-CH}_3\text{COO})_2\text{ML}]^{2+}$  ( $\text{M} = \text{Fe}(\text{II})$  or  $\text{Co}(\text{II})$ ), uncoordinated perchlorate anions, and water of crystallization. The metal centers Cr(III) and Fe(II) or Co(II) are linked together via a hydroxo bridge and two further acetate bridges; the geometry around each metal center is distorted octahedral. The perchlorate salts of other heterodinuclear complexes are isostructural with the Cr(III)-Fe(II) and Cr(III)-Co(II) complexes. They also crystallize in the triclinic system, space group  $C_1^1\text{-P}\bar{1}$ , with very similar unit cell dimensions. Variable-temperature (4–300 K) magnetic susceptibility measurements indicate that the spins of Cr(III) and M(II) or Cr(III) are weakly antiferromagnetically coupled. The electronic spectra have been measured both in the solid state and in solution, and they are very similar, indicating the presence of the stable moiety  $[\text{Cr}^{\text{III}}(\mu\text{-OH})(\text{CH}_3\text{COO})_2\text{M}]^{2+}$ , also in solution. The spin-flip  ${}^4\text{A}_{2g} \rightarrow {}^2\text{E}_g$  transitions with intensity gain from exchange coupling have been observed for the homodinuclear Cr(III)-Cr(III) complex. Redox potentials for the couples Cr(III)-M(III)/Cr(III)-M(II) ( $\text{M} = \text{Mn}, \text{Fe},$  or  $\text{Co}$ ) vs.  $\text{Fe}^+/\text{Fe}^0$  ( $\text{Fe}^0 = \text{ferrocene}$ ) have been determined from their quasi-reversible cyclic voltammograms (+0.36, -0.05, and +0.03 V, respectively) in acetonitrile.

### Introduction

Both homo- and heterodinuclear transition-metal complexes occupy an important position in modern inorganic chemistry. The impetus for the study of these complexes derives from the interests in connection with magnetic exchange interactions<sup>1-4</sup> and electron

transfer between metal ions<sup>5</sup> and from their significance as models<sup>6,7</sup> for biological systems. New magnetic exchange path-

- (1) *Magneto-Structural Correlations in Exchange Coupled Systems*; Willett, R., Gatteschi, D., Kahn, O., Eds.; NATO ASI Series C: Mathematical and Physical Science; Reidel: Dordrecht, The Netherlands, 1985; Vol. 140.
- (2) Kahn, O. *Angew. Chem.* **1985**, *97*, 837-853.
- (3) Timken, M. D.; Marritt, W. A.; Hendrickson, D. N.; Gagne, R. A.; Sinn, E. *Inorg. Chem.* **1985**, *24*, 4202-4208.

\* Ruhr-Universität.

† Anorganisch Chemisches Institut der Universität Heidelberg.